

OPEN

# Intranasal Orexin After Cardiac Arrest Leads to Increased Electroencephalographic Gamma Activity and Enhanced Neurologic Recovery in Rats

**OBJECTIVES:** Prolonged cardiac arrest is known to cause global ischemic brain injury and functional impairment. Upon resuscitation, electroencephalographic recordings of brain activity begin to resume and can potentially be used to monitor neurologic recovery. We have previously shown that intrathecal orexin shows promise as a restorative drug and arousal agent in rodents. Our goal is to determine the electrophysiology effects of orexin in a rodent model of asphyxial cardiac arrest, focusing on the electroencephalographic activity in the gamma and super-gamma bands (indicative of return of higher brain function).

**DESIGN:** Experimental animal study.

**SETTING:** University-based animal research laboratory.

**SUBJECTS:** Adult male Wistar rats.

**INTERVENTIONS:** In an established model of asphyxial cardiac arrest ( $n = 24$ ), we treated half of Wistar rats with orexin administered intranasally by atomizer 30 minutes post return of spontaneous circulation in one of two dose levels (10 and 50  $\mu\text{M}$ ); the rest were treated with saline as control. Continuous electroencephalographic recording was obtained and quantitatively analyzed for the gamma fraction. Gamma and high-frequency super-gamma band measures were compared against clinical recovery according to Neuro-Deficit Score.

**MEASUREMENTS AND MAIN RESULTS:** Compared with the control cohort, the high-dose orexin cohort showed significantly better Neuro-Deficit Score 4 hours after return of spontaneous circulation (55.17 vs 47.58;  $p < 0.02$ ) and significantly higher mean gamma fraction (0.251 vs 0.177;  $p < 0.02$ ) in cerebral regions surveyed by rostral electrodes for the first 170 minutes after administration of orexin.

**CONCLUSIONS:** Our findings support early and continuous monitoring of electroencephalography-based gamma activity as a marker of better functional recovery after intranasal administration of orexin as measured by Neuro-Deficit Score in an established animal model of asphyxial cardiac arrest.

**KEY WORDS:** asphyxia; brain injury; cardiac arrest; neurologic dysfunction; outcome prediction

Hypoxic encephalopathy is present in most patients resuscitated following cardiorespiratory arrest (1); in most patients, it is followed by persistent neurologic disorder of consciousness, cognitive dysfunction, or death (2–4). Within seconds of cardiac arrest, electroencephalography

David L. Sherman, PhD<sup>1</sup>

Autumn Williams, MS<sup>1</sup>

Sahithi GD, PhD<sup>1</sup>

Hiren R. Modi, PhD<sup>1</sup>

Qihong Wang, PhD<sup>1</sup>

Nitish V. Thakor, PhD<sup>1</sup>

Romergrzyko G. Geocadin, MD<sup>2</sup>

Copyright © 2021 The Authors. Published by Wolters Kluwer Health, Inc. on behalf of the Society of Critical Care Medicine. This is an open-access article distributed under the terms of the Creative Commons Attribution-Non Commercial-No Derivatives License 4.0 (CCBY-NC-ND), where it is permissible to download and share the work provided it is properly cited. The work cannot be changed in any way or used commercially without permission from the journal.

DOI: 10.1097/CCE.0000000000000349

is suppressed (5) and recovers via periodic bursting, progressing to restitution of continuous activity (6, 7). In acute brain injuries, clinical analyses of electroencephalographic frequencies have been limited to traditional frequencies (delta, theta, alpha, and beta) (8–10)—although these frequencies represent return of basic brain function, frequencies in the gamma range represent the neural activity we associate with learning, memory, emotions, and behavioral planning (8–10).

Orexin is a hypothalamic neuropeptide (11) showing anti-neuroinflammatory (12) and arousal effects (13) and is involved in blood pressure regulation (14). It is negatively impacted by traumatic brain injury (15–17). Intraventricular administration of orexin results in improvements in recovery following brain injury (16, 18) and cardiac arrest (13, 14). The translational value of this work is limited due to the invasive nature of intraventricular administration; however, intranasal delivery is a safer method with similar drug delivery potential (17, 19), and intranasal orexin has been found to alleviate cognitive deficits due to aging (20), narcolepsy (21), and sleep deficit (22). This motivated us to explore the effects of intranasal orexin on recovery post cardiac arrest using electroencephalography as a biomarker.

In our experimental studies on a rodent model, we found that intranasally delivered orexin promoted postcardiac arrest arousal (14). As evidence, we observed that electroencephalography showed an increase in the fraction of gamma band power over total power or gamma fraction (G-FRAC). In the current work, we expand our definition of G-FRAC to examine both the gamma and super-gamma frequency ranges and modify our algorithm to more accurately approximate and dissect the electroencephalographic signals in animals with and without orexin treatment. We insure that we use an expanded wavelet-defined spectral power description. Our earlier methodology using sinusoidal energy measurements did not accurately describe power in the gamma band (14). Gamma in particular is a notably wide band that lends itself to wavelet-based power measurements. We test the hypothesis that the quantitative examination of gamma range activity will allow us to identify favorable functional outcomes resulting from enhanced neurologic recovery with intranasal orexin.

## MATERIALS AND METHODS

### Experimental Protocol

All experimental procedures were conducted in accordance with the National Resource Council's guidelines for the care and use of laboratory animals (23). Our studies on asphyxial cardiac arrest (24, 25) and cardiopulmonary resuscitation (CPR) (15, 16) were approved by the Animal Care and Use Committee of the Johns Hopkins Medical Institutions (protocol number RA19M498).

Rats were endotracheally intubated with a 14 G catheter (TERUMO Surfash IV catheter) and mechanically ventilated with 2% isoflurane (Baxter, Chicago, IL) in 50% oxygen and 50% nitrogen gas at 35 breaths per minute by a rodent ventilator (Harvard Apparatus model 553438). Ventilation was adjusted to maintain physiologic pH,  $PO_2$ , and  $PCO_2$ . Body temperature was maintained at  $37.0^\circ C \pm 0.5^\circ C$  throughout the experiment. The left femoral artery and vein were cannulated with polyethylene 50 tubing catheters (Intramedic Non-Radiopaque Polyethylene Tubing PE 50; Becton Dickinson, Franklin Lakes, NJ) to continuously monitor mean arterial pressure, intermittently sample arterial blood gas, and administer fluid and drugs. Arterial blood gas samples were measured by an i-STAT handheld analyzer (Abbott Point of Care Inc, Princeton, NJ). After 10 minutes of baseline recording, isoflurane was discontinued for 5 minutes to ensure no significant residual effect on electroencephalography, and vecuronium bromide 2 mg/kg IV (Novaplus; Abbott Labs, North Chicago, IL) was infused. No sedative or anesthetic agents were administered throughout the remainder of the experiment to avoid confounding effects on electroencephalography. Cardiac arrest was initiated via asphyxia by stopping and disconnecting the ventilator and clamping the tracheal tube for 7 minutes. Cardiac arrest was defined by pulse pressure less than 10 mm Hg and asystole. CPR was performed with unclamping of the tracheal tube, resumption of ventilation and oxygenation (100%  $FIO_2$ ), infusion of epinephrine (5  $\mu g/Kg$ , IV) and  $NaHCO_3$  (1 mmol/Kg, IV), sternal chest compressions (200/min) until return of spontaneous circulation (ROSC), and showing mean arterial pressure greater than 50 mm Hg and pulse waveform. Ventilator adjustments were performed according to the arterial blood gas findings. The animals were allowed to recover spontaneously after resuscitation

and, subsequently, were extubated along with removal of all invasive catheters. The rats had free access to food and water before and after the experiments and were housed in a quiet environment with a 12-hour day-night cycle.

Twenty-four adult male Wistar rats (300–350g; Charles River, Wilmington, MA) were given 7-minute asphyxial cardiac arrest and then resuscitated. The rats were randomly assigned to one of three groups: 10  $\mu$ M orexin (orexin-10 cohort;  $n = 6$ ), 50  $\mu$ M orexin (orexin-50 cohort;  $n = 6$ ), or saline vehicle as control (control cohort;  $n = 12$ ). At 30 minutes post ROSC, each rat received the intranasal dose corresponding to their group over a 30-second interval. To reduce potential bias, neuromonitoring data collected from rats were deidentified, and analysis of electroencephalographic data was performed by researchers who had neither involvement in the experimental protocol nor any contact with the rats themselves. Following the neuromonitoring observation period, all rats were destroyed, and thus no follow-up or survival rate data was collected.

## Data Collection

Four channels of electroencephalography were recorded using epidural screw electrodes (Plastics One, Roanoke, VA) from baseline throughout the recovery period. Rostral electrodes were placed laterally equidistant from the bregma and anterior to the coronal suture, whereas caudal electrodes were placed laterally equidistant from the lambda (Fig. 1). The signals were digitized using the TDT-System 3 data acquisition

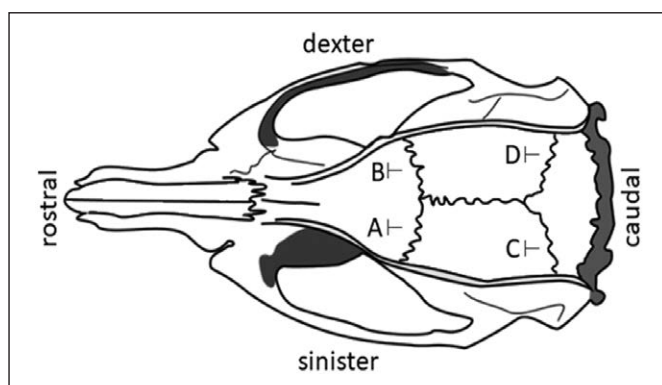


**Figure 1.** Approximate placement of electrodes on Wistar rat subjects. Sinistrorostral (A) and dextrorostral (B) electrodes were placed laterally equidistant from the bregma and anterior to the coronal suture; sinistrocaudal (C) and dextrocaudal (D) electrodes were placed laterally equidistant from the lambda and anterior to the lambdoid suture.

package (Tucker-Davis Technologies NC., Alachua, FL). A sampling frequency of 12,207 Hz with 12-bit A/D conversion (Tucker-Davis Technologies) was used. Raw electroencephalography was down-sampled by 50 $\times$  in three distinct steps (2 $\rightarrow$ 5 $\rightarrow$ 5) and reviewed for movement artifact and signal quality; artifact-ridden epochs were removed prior to analysis. One subject in the orexin-10 group experienced a fault in the sinistrorostral electrode, and this single electrode was discarded from analysis. To limit interference from the local electrical environment, the 59–61 Hz frequency was filtered out of all electroencephalographic recordings using a second order Butterworth notch filter fit to the final target sample rate of 244 Hz.

## Quantitative Electroencephalography

We used the discrete wavelet transform to calculate band power to break the electroencephalography signal into its coarse and fine feature bands, which provides a cleaner separation than our previous method and maps well to the electroencephalographic frequency bands of interest. Further, we used here a ninth order Symlets basic wavelet, notable for its high cross-correlation with stable parietal electroencephalography (26), permitting this method to model the electroencephalographic waveform more accurately than the sinusoids of our prior work (12).

We divided the recording from each electrode from each subject into sets of 10 seconds and then used a 1D, five-level dyadic wavelet decomposition to estimate coefficients of the underlying wavelet. Based on our sampling rate of 244 Hz per channel, this method of decomposition results in the frequency ranges of each of the resulting detail levels approximating the standard frequency bands of clinical relevance in the analysis of electroencephalography: (super-gamma: 61.5–122 Hz, gamma: 30.75–61.5 Hz, beta: 15.375–30.75 Hz, alpha: 7.688–15.375 Hz, theta: 3.844–7.688 Hz, and delta: 1.922–3.844 Hz). This shows the value of the wavelet decomposition in that it separates the frequency bands of interest as a consequence of the calculation (27).

Once we determined the wavelet coefficients at each band level,  $W$ , we calculated the power in each band by taking the square of the sum of the absolute values of the wavelet coefficients for each band level,  $|W_i|^2$ . G-FRAC is then calculated by dividing the sum of the gamma and super-gamma band powers by the total band power for each time point.

$$\text{GFRAC} = \frac{|W_{\gamma}|^2 + |W_{\gamma<}|^2}{\sum |W_i|^2} \quad (\text{Eq 1})$$

Values of G-FRAC in six 10-second periods were averaged together unweighted to estimate the G-FRAC of each minute.

## Neuro-Deficit Score

The Neuro-Deficit Score (NDS) quantifies the level of consciousness, awareness, and neurologic function of a rat, similar to the use of the Glasgow Coma Score in humans. In our prior work, this was used to illustrate the separation of good and poor outcome classes (29–31). It ranges from 0 (deceased) to 80 (completely healthy), with measures of consciousness and arousal (General Behavior Subscore, GBS); reflexes, vision, and stimulus response (Brain stem Function Subscore, BFS); as well as motor function, behavior, and other neurologic function or dysfunction. Each subject was assessed with the NDS rubric (29) at 4 hours post ROSC. In order to verify the impact of the discrete categories of orexin dose level on the resulting neurologic function, we grouped these data by cohort, assessing the pairwise differences between the control cohort and each of the orexin cohorts' means using the Wilcoxon rank-sum test and between the cohorts' SDs using the *F* test of equal variances. For groups that showed significant differences, we applied a binomial logistic regression to assess the level at which binary cohort assignment (0 or 1) between them could be predicted based on NDS. We performed the following sequence to evaluate the relationship between G-FRAC and NDS:

- 1) Divided monitoring period into increments of 5 minutes.
- 2) Calculated a battery of statistical measures for this period.
- 3) Calculated Pearson correlation coefficient of each measure against the NDS values of the subject.
- 4) Repeated test for increasing 5-minute time increments and compare calculations.

We also repeated this process for the gamma-only and super-gamma-only fractions of the total band power.

## RESULTS

### Effects of Orexin on NDS

Values for GBS ranged from 11 to 19 for both the overall and control cohorts, 14–19 for both orexin cohorts; for

BFS, from 9 to 21 for overall and orexin-50 cohort, 12–21 for control and orexin-10 cohorts. Overall NDS ranged from 38 to 59; control cohort ranged from 39 to 55, mean  $47.6 \pm 4$ ; orexin-10 cohort 38–58, mean  $46.7 \pm 7.6$ ; orexin-50 cohort 43–59, mean  $55.2 \pm 6.11$ . We display these data in **Table 1**, broken into the GBS, BFS, and the overall NDS; the two subscores listed account for 50–70% of the total NDS value of each subject.

Cohorts did not show significant differences on SD for either subscore or NDS at 5% alpha level. Cohorts did not show any significant difference on mean of individual subscores. A significant difference on total NDS was found only between the control and orexin-50 groups ( $p < 0.02$ ).

Only one subject, which was in the orexin-50 cohort, received a BFS below 12. Based on an assessment of brainstem function showing poor restoration of reflexes in response to stimuli, resulting in dramatically lower NDS, we identified this subject as a potential outlier in terms of either level of injury or treatment response. To compensate for this, we performed all cohort-level analyses involving the orexin-50 group both including and excluding this subject; effects of this exclusion are noted where appropriate.

At least one subject in each cohort received the maximum possible score for GBS; the same can be said for BFS. The highest score received for NDS was 59 of a possible 80. Both the constant and coefficient of the predictive equation for the binomial logistic regression between the control and orexin-50 cohorts based on NDS had acceptable significance ( $p < 0.03$ ; SD 15.69):

$$P = \left(1 + e^{17.5864 - 0.3281 \times \text{NDS}}\right)^{-1} \quad (\text{Eq 2})$$

Since no significant difference was found between the mean values of NDS for the control and orexin-10 cohorts, a regression would not be statistically valid and thus was not performed.

### Effects of Orexin on G-FRAC

We began our examination by combining measurements of all subjects in each cohort to obtain an average G-FRAC per minute by cohort (**Fig. 2**). This provides a clear image that the G-FRAC for the orexin-50 cohort differed noticeably from the G-FRAC for both the control and orexin-10 cohorts; although the control and orexin-10 cohorts' mean G-FRAC values trace a



**TABLE 1.**  
**Descriptive Statistics for Neuro-Deficit Score and Primary Subscores**

Cohort	n	General Behavior Subscore				Brainstem Function Subscore				Neuro-Deficit Score			
		Minimum	Mean	Maximum	SD	Minimum	Mean	Maximum	SD	Minimum	Mean	Maximum	SD
Overall	24	11	16.3	19	2.9	9	16.5	21	3.8	38	49.3	59	6.4
control	12	11	16.2	19	3.2	12	15.5	21	3.3	39	47.6	55	4.0
Orexin-10	6	14	14.8	19	2.0	12	16.5	21	3.1	38	46.7	58	7.6
Orexin-50	6	14	18.2	19	2.0	9	18.5	21	4.8	43	55.2	59	6.11

Table of descriptive statistics for the General Behavior Subscore, containing consciousness and arousal; Brainstem Function Subscore, for reflexes, vision, and other physical response to stimuli; and the overall Neuro-Deficit Score (NDS), both for all subjects and for each of the three experimental cohorts—control saline, low-dose orexin (orexin-10), and high-dose orexin (orexin-50). The orexin-50 cohort shows a significantly higher mean NDS ( $p < 0.02$ ) per the Wilcoxon rank-sum test than the control cohort, whereas no significant difference was measured between control and orexin-10. As even a single point loss on NDS can represent marked loss of function, with three points generally indicating total absence of a major bodily function, a difference of this magnitude is indicative of a pronounced difference in outcome. This supports our hypothesis of the therapeutic potential for intranasal administration of orexin to improve neurologic recovery at an appropriate dosage level.

similar path, the orexin-50 cohort shows a dramatic rise immediately from administration and continues at this level through the neuromonitoring period. The control and orexin-10 cohort measures only catch up to the orexin-50 cohort measures at approximately 180 minutes post ROSC (150 min post administration).

Our next step was to compare each scalp location (electrode placement) within each cohort to assess whether specific cerebral regions showed greater response to treatment with orexin. If certain cerebral regions responded more strongly, we would see greater differences in G-FRAC between the control cohort

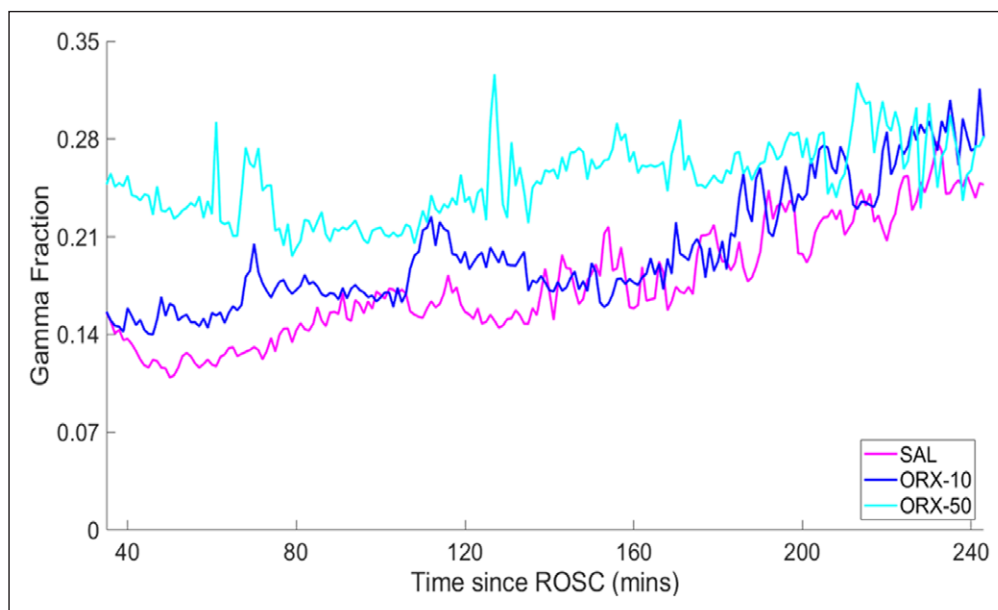


**Figure 2.** Mean gamma fraction (G-FRAC) for all subjects in each cohort per minute. Orexin dose was administered intranasally at 30 min after return of spontaneous circulation (ROSC), and subjects were monitored continuously until 240 min after ROSC. *Magenta line* represents Control Saline (SAL) cohort, which received no orexin; *blue line*, orexin-10 (ORX-10) cohort, which received 10  $\mu\text{M}$  of orexin; *cyan line*, orexin-50 (ORX-50) cohort, which received 50  $\mu\text{M}$ . Although the G-FRAC for control and ORX-10 follows a similar pattern, the ORX-50 cohort shows a dramatic rise from the point of administration that remains steadily above the other cohorts. We examine the reason for this difference further in the next figure.

and the orexin cohorts in electrodes surveying those regions (**Fig. 3**). Under both caudal electrodes, all three cohorts displayed similar behavior for mean G-FRAC; the orexin-50 measurements diverge substantially from the other two cohorts only in the rostral electrodes. Further, the sinistrorostral electrode (labeled A in Fig. 1) accounts for the largest difference between the orexin-50 cohort and the orexin-10 and control cohorts, both in terms of actual difference and for the longest period. We confirmed the intracohort electrode differences in this measurement by

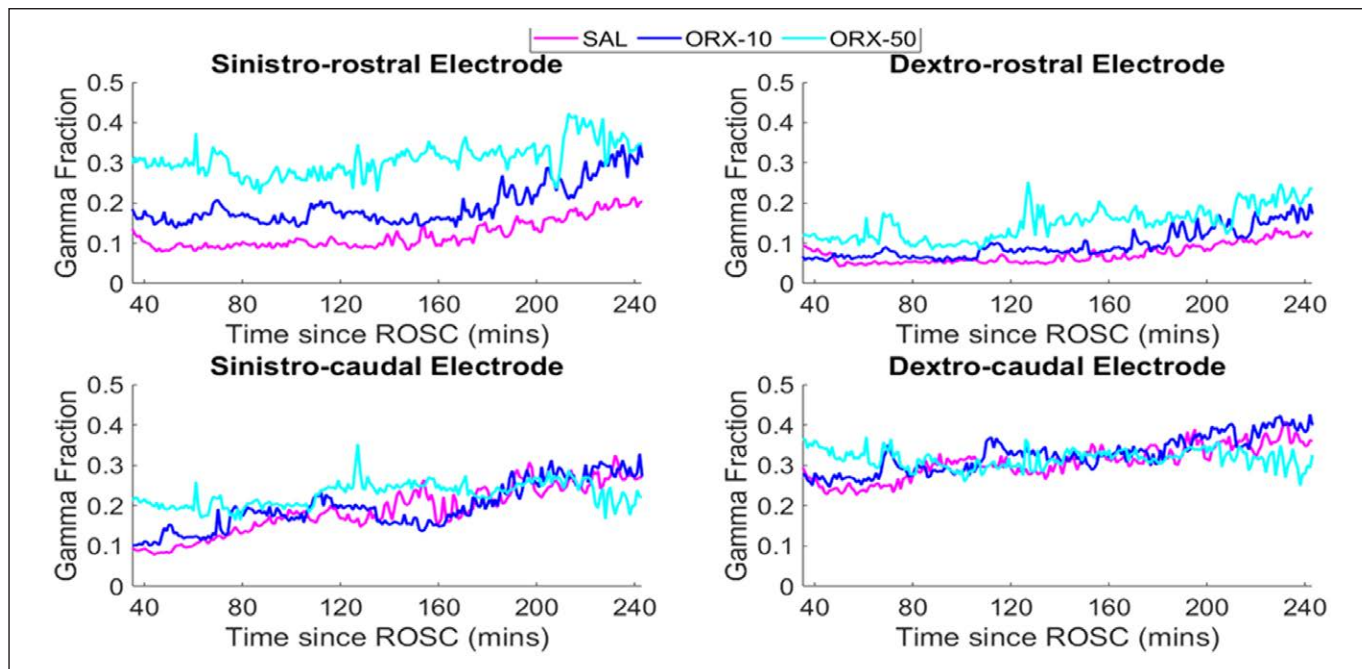


**Figure 3.** Mean gamma fraction (G-FRAC) per minute values averaged over subjects in each cohort for each separate electrode. Lines in magenta indicate the specified electrode in the control cohort, lines in blue for the orexin-10 (ORX-10) cohort, lines in cyan for the orexin-50 (ORX-50). See Figure 1 for diagram of electrode positions. In the two bottom graphs (caudal electrodes), all three cohorts display similar behavior. In the top left (sinistrorostral), we see the largest gap between the ORX-50 and ORX-10 groups for much of the monitored period. This suggests that the cerebral region surveyed by the sinistrorostral electrode is the site where the effect of the orexin dose is most felt during neurologic recovery. This is further supported by the fact that the top right (sinistrorostral electrode) graph is also where we see the largest gap between the ORX-10 and control groups, indicating that a dose level below clinical effectiveness in terms of neurologic recovery still has a noticeable effect on the level of cerebral activity occurring in the region surveyed by this electrode. SAL = saline.

examining the Pearson correlation between the different electrodes (Table 2).

The intracohort electrode correlations (Table 2) reinforce differences seen in Figure 3. For the control and orexin-10 cohorts, we see high intracohort correlations between electrodes (from 0.74 to 0.97;  $p < 0.001$ ), indicating a high degree of synchrony between different cerebral regions. With the exception of the correlation between the two rostral electrodes however, the intracohort correlations for the orexin-50 electrodes are drastically lower (from 0.26 to 0.56;  $p < 0.001$ ) showing a large effect of orexin on gamma and super-gamma band activity in the higher dose group; even the two rostral electrodes show only a correlation of 0.79, barely more than the lowest correlation found in the other two cohorts.

In comparison with the control cohort, the sinistrorostral electrodes of the orexin-50 cohort show significantly higher G-FRAC values for minimum (0.093 vs 0.052;  $p < 0.02$ ), mean (0.308 vs 0.121;  $p < 0.02$ ), and mean area-under-curve (64.07 vs 25.05;  $p < 0.02$ ),

which establishes that the higher values are a trend and not isolated points. These comparisons were not significant ( $p > 0.1$ ) when examining the gamma-only or super-gamma-only fractions.

### Relationship Between NDS and G-FRAC

Our comparison of the correlations from the overall and sinistrorostral electrode for the expanded G-FRAC of the control and orexin-50 cohorts to the NDS found acceptable significance ( $p < 0.05$ ) for the linear-fit derivative measure for most of the increasing time increments, especially 110 minutes post ROSC and later. Values ranged from  $-0.47$  to  $-0.59$  for overall and  $-0.47$  to  $-0.63$  for the sinistrorostral electrode. Relative measures approaching significance ( $0.05 < p < 0.1$ ) for several increments included mean, Euclidean distance, interquartile range, and kurtosis. Correlations of all measures were not found to be significant for the gamma- or super-gamma-only fractions of total band power ( $p > 0.05$ ), with the closest item being the gamma-only fraction for mean ( $0.05 < p < 0.1$ ).

**TABLE 2.**  
**Intracohort Correlations by Electrode**

Cohort	n	Electrode			
Overall	24		B	C	D
		A	0.967	0.787	0.836
		B		0.825	0.870
		C			0.948
Control	12		B	C	D
		A	0.961	0.815	0.838
		B		0.7356	0.777
		C			0.944
Orexin-10	6		B	C	D
		A	0.950	0.840	0.845
		B		0.876	0.906
		C			0.896
Orexin-50	6		B	C	D
		A	0.798	0.434	0.396
		B		0.562	0.262
		C			0.442

Intracohort Pearson correlations of mean gamma fraction (G-FRAC) per minute for each separate electrode, averaged for all subjects and over subjects in each cohort. All values significant at  $p < 0.001$  for two-tailed t test. Control cohort received no orexin; orexin-10 cohort received 10  $\mu\text{M}$  of orexin; orexin-50 cohort received 50  $\mu\text{M}$  of orexin. Note orexin-10 cohort includes only five subjects for measures of A (sinistrostral electrode) as one subject in this cohort had a single faulty electrode (see *Data Collection* section). Cell at (row, col) = (X, Y) of this table indicate level of correlation between electrodes X and Y for mean G-FRAC per minute. See Figure 1 for the positions of electrodes by labeling. The correlation between the rostral (A, B) and caudal (C, D) electrodes is high in the control and orexin-10 cohorts; however, it drops precipitously in the orexin-50 cohort. Only the two rostral (A, B) electrodes maintain a semblance of correlation with each other for orexin-50, and even then, it is lower than in the control or orexin-10 cohorts. The markedly lower coherence between cerebral regions in the orexin-50 cohort lends further support to the evidence presented in Figure 2 that there is a differential response by cerebral region to the administered orexin.

## DISCUSSION

Our results support our hypothesis that inclusion of both the gamma and super-gamma frequency ranges in the quantitative electroencephalography (qEEG)

monitoring provide better identification of animals experiencing more favorable neurologic outcomes than the gamma frequency range alone. Not only was the separation between the treatment groups of greater significance using both ranges together but also the combined frequency fraction showed significant correlation to the NDS on more measures.

The values of the binomial logistic regression between the control and orexin-50 cohorts indicate a moderate support for increased NDS to signify the high dose was received rather than the control saline. Together with the finding in Figure 2 that the orexin-50 cohort outpaces the rise in the other cohorts, this provides early evidence that administration of orexin leads to arousal detected by G-FRAC and the potential for increased neurologic recovery in the subjects of the orexin-50 cohort. When examining the cerebral regions, we found that the difference between the cohorts is mainly in the region implicated in sensorimotor function and spatial memory in rats (28), in agreement with our understanding that differences in the gamma band are primarily in regions related to more complex thought processes.

Our statistical comparison shows that NDS of the orexin-50 cohort is significantly higher than for the control cohort. As even a single point difference in NDS value can be indicative of a significant loss of function in terms of sensation, responsiveness, or motor capability, a significant difference with a magnitude of seven points shows a major disparity in functional outcome between the two groups. G-FRAC for orexin-50 rose shortly after administration, which only occurred to the control cohort hours later. The late increase in band power values is not reflected in the animals' neurologic recovery profiles; this supports our earlier contention that there is a limited window for intervention to aid in neurologic recovery. Based on our correlational assessment, the flatness of the control G-FRAC is also a matter of concern; the moderate negative correlation with linear-fit derivative indicates that sharp, slow increases are not helpful to recovery, whereas short-term variations with underlying preservation of stability are more indicative of healthy future outcome—especially if we consider the implications of the less significant measures in showing a positive effect of a broad range of values over a short time span.

What this study does suggest is the practical benefit to assessment of neurologic recovery through

examination of the qEEG gamma and super-G-FRAC. Having verified that the orexin-50 cohort differs significantly from the control cohort in NDS and that the effect of orexin on G-FRAC is principally observed in the sinistorostral electrode, our final goal was to examine whether G-FRAC can be used to predict NDS; this would provide support for the use of G-FRAC as a biomarker that could be used to assess a subject's recovery potential. Although our previous studies (12, 14, 24, 25, 30) showed the accuracy of using qEEG and G-FRAC to distinguish known groups, this study provides an avenue to examine effectiveness of treatment in medical research—to identify which functional outcome a patient is currently heading toward, based on the shape and qualities of the G-FRAC they currently present. Our goal in this investigation is to provide a set of assessment criteria that a medical device could apply to electroencephalographic readings that would have sufficient predictive power to track clinical changes related to different treatment levels.

The primary limitation of this study was the division of cohorts: our analysis found no significant effect of the lower dose, and the reduced sample size resulting from two different levels of treatment reduced the statistical power of the experiment to a precarious level. Given the magnitude of difference between the low- and high-dose groups, we do not believe it would be statistically valid to combine the two and instead look to a future experiment with a larger sample size and fewer comparisons. There were several measures we examined in the high-dose cohort for which a slight increase to statistical power could have brought clearer distinction as to their level of significance. Further, the level of dispersion—how focused a signal is—is a commonality of the statistical measures we found to be potentially significant if examined at higher power. Being able to identify how concentrated the signal is could allow us to pinpoint the kind of neural activity occurring in the subject and in turn identify what stage of the recovery process the subject is undergoing at a given time. The volatility in the signal could also be used to assess the level of restoration of proper function by comparison with the background activity that we would expect in normal function. We plan to examine this property in a future study. Other potential features for future exploration include different shapes of the waveforms of the biomarker measure, additional doses (rather than dose levels), and further

specification of cerebral regions to better pinpoint the center of the effect.

## CONCLUSIONS

These findings show intranasal orexin's translational potential to enhance neurologic and behavioral recovery of patients postcardiac arrest. We demonstrated this through the selected 50  $\mu$ M therapeutic dose of orexin using a noninvasive method of administration, nasal delivery for increased clinical applicability, and pairing with qEEG technique, especially G-FRAC as the indicator to monitor patient recovery trajectories.

1 Department of Biomedical Engineering, Johns Hopkins University, Baltimore, MD.

2 Departments of Neurology, Anesthesiology-Critical Care Medicine, and Neurosurgery, Johns Hopkins University School of Medicine, Baltimore, MD.

The authors have disclosed that they do not have any potential conflicts of interest.

For information regarding this article, E-mail: [dvdsherman@gmail.com](mailto:dvdsherman@gmail.com)

## REFERENCES

1. Neumar RW, Nolan JP, Adrie C, et al: Post-cardiac arrest syndrome: Epidemiology, pathophysiology, treatment, and prognostication. A consensus statement from the International Liaison Committee on Resuscitation (American Heart Association, Australian and New Zealand Council on Resuscitation, European Resuscitation Council, Heart and Stroke Foundation of Canada, InterAmerican Heart Foundation, Resuscitation Council of Asia, and the Resuscitation Council of Southern Africa); the American Heart Association Emergency Cardiovascular Care Committee; the Council on Cardiovascular Surgery and Anesthesia; the Council on Cardiopulmonary, Perioperative, and Critical Care; the Council on Clinical Cardiology; and the Stroke Council. *Circulation* 2008; 118:2452–2483
2. Wijdicks E: Anoxic ischemic encephalopathy. In: *Prognosis in Neurology*. Gilchrist J (Ed). Boston, MA, Butterworth Heinemann, 1998, pp 7–10.
3. Geocadin RG, Koenig MA, Jia X, et al: Management of brain injury after resuscitation from cardiac arrest. *Neurol Clin* 2008; 26:487–506, ix
4. Geocadin R: Understanding and enhancing functional outcomes after cardiac arrest: The need for a multidisciplinary approach to refocus on the brain. *Resuscitation* 2009; 80:153–154
5. Edgren E, Hedstrand U, Kelsey S, et al: Assessment of neurological prognosis in comatose survivors of cardiac arrest. BRCT I Study Group. *Lancet* 1994; 343:1055–1059



6. Jørgensen EO, Malchow-Møller A: Natural history of global and critical brain ischaemia. Part I: EEG and neurological signs during the first year after cardiopulmonary resuscitation in patients subsequently regaining consciousness. *Resuscitation* 1981; 9:133–153
7. Jørgensen EO, Malchow-Møller A: Natural history of global and critical brain ischaemia. Part II: EEG and neurological signs in patients remaining unconscious after cardiopulmonary resuscitation. *Resuscitation* 1981; 9:155–174
8. Brovelli A, Lachaux JP, Kahane P, et al: High gamma frequency oscillatory activity dissociates attention from intention in the human premotor cortex. *Neuroimage* 2005; 28:154–164
9. Lachaux JP, Axmacher N, Mormann F, et al: High-frequency neural activity and human cognition: Past, present and possible future of intracranial EEG research. *Prog Neurobiol* 2012; 98:279–301
10. Müsch K, Hamamé CM, Perrone-Bertolotti M, et al: Selective attention modulates high-frequency activity in the face-processing network. *Cortex* 2014; 60:34–51
11. Mihara Y, Dohi K, Yofu S, et al: Expression and localization of the orexin-1 receptor (OX1R) after traumatic brain injury in mice. *J Mol Neurosci* 2011; 43:162–168
12. Koenig MA, Jia X, Kang X, et al: Intraventricular orexin-A improves arousal and early EEG entropy in rats after cardiac arrest. *Brain Res* 2009; 1255:153–161
13. Kang YJ, Tian G, Bazrafkan A, et al: Recovery from coma post-cardiac arrest is dependent on the orexin pathway. *J Neurotrauma* 2017; 34:2823–2832
14. Modi HR, Wang Q, Gd S, et al: Intranasal post-cardiac arrest treatment with orexin-A facilitates arousal from coma and ameliorates neuroinflammation. *PLoS One* 2017; 12:e0182707
15. Baumann CR, Bassetti CL, Valko PO, et al: Loss of hypocretin (orexin) neurons with traumatic brain injury. *Ann Neurol* 2009; 66:555–559
16. Dong XY, Feng Z: Wake-promoting effects of vagus nerve stimulation after traumatic brain injury: Upregulation of orexin-A and orexin receptor type 1 expression in the prefrontal cortex. *Neural Regen Res* 2018; 13:244–251
17. Dhuria SV, Hanson LR, Frey WH 2nd: Intranasal drug targeting of hypocretin-1 (orexin-A) to the central nervous system. *J Pharm Sci* 2009; 98:2501–2515
18. Jia XB, Li LS, Ye JN, et al: Study on arousal effect of orexin-A in rat in coma due to ischemic brain injury. *Crit Care Med China* 2008; 20:361–364
19. Liu X: Clinical trials of intranasal delivery for treating neurological disorders—a critical review. *Expert Opin Drug Deliv* 2011; 8:1681–1690
20. Calva CB, Fadel JR: Intranasal administration of orexin peptides: Mechanisms and therapeutic potential for age-related cognitive dysfunction. *Brain Res* 2020; 1731:145921
21. Weinhold SL, Seeck-Hirschner M, Nowak A, et al: The effect of intranasal orexin-A (hypocretin-1) on sleep, wakefulness and attention in narcolepsy with cataplexy. *Behav Brain Res* 2014; 262:8–13
22. Deadwyler SA, Porrino L, Siegel JM, et al: Systemic and nasal delivery of orexin-A (Hypocretin-1) reduces the effects of sleep deprivation on cognitive performance in nonhuman primates. *J Neurosci* 2007; 27:14239–14247
23. Council NR: *Guide for the Care and Use of Laboratory Animals*. Washington, DC, Natl Academies Press, 2011
24. Jia X, Koenig MA, Shin HC, et al: Quantitative EEG and neurological recovery with therapeutic hypothermia after asphyxial cardiac arrest in rats. *Brain Res* 2006; 1111:166–175
25. Jia X, Koenig MA, Shin HC, et al: Improving neurological outcomes post-cardiac arrest in a rat model: Immediate hypothermia and quantitative EEG monitoring. *Resuscitation* 2008; 76:431–442
26. Al-Qazzaz NK, Bin Mohd Ali SH, Ahmad SA, et al: Selection of mother wavelet functions for multi-channel EEG signal analysis during a working memory task. *Sensors (Basel)* 2015; 15:29015–29035
27. Paul JS, Patel CB, Al-Nashash H, et al: Prediction of PTZ-induced seizures using wavelet-based residual entropy of cortical and subcortical field potentials. *IEEE Trans Biomed Eng* 2003; 50:640–648
28. Zhai Z, Feng J: Left-right asymmetry influenced the infarct volume and neurological dysfunction following focal middle cerebral artery occlusion in rats. *Brain Behav* 2018; 8:e01166
29. Geocadin RG, Muthuswamy J, Sherman DL, et al: Early electrophysiological and histologic changes after global cerebral ischemia in rats. *Mov Disord* 2000; 15 (Suppl 1):14–21
30. Geocadin RG, Ghodadra R, Kimura T, et al: A novel quantitative EEG injury measure of global cerebral ischemia. *Clin Neurophysiol* 2000; 111:1779–1787
31. Geocadin RG, Sherman DL, Christian Hansen H, et al: Neurological recovery by EEG bursting after resuscitation from cardiac arrest in rats. *Resuscitation* 2002; 55:193–200